Evidence for Ionic Diffusion in Dynamic Light Scattering from Glass-forming Sodium Borate Melts

H. G. Uppala and D. L. Sidebottom

Dept. of Physics, Creighton University

Abstract

Photon correlation spectroscopy conducted on glass-forming sodium borate melts provides a measure of the dynamic structure factor of these network-forming liquids over a broad time window and large temperature range. The dynamics are complex and include a non-Arrhenius temperature dependence and a non-exponential response to perturbations both of which are observed in the present measurements and both of which evolve with changes in the density of covalent bonds. An unexpected feature is the occurrence of a second, much slower relaxation process that develops only in the sodium-modified borates with up to 10 mol% sodium oxide. This second process appears to be caused by the diffusion of sodium ions as they undergo random ion hopping between charge-compensating sites in the network on a timescale equal to that of the viscous relaxation.

I. Introduction

The dynamics in supercooled glass-forming liquids become increasingly complex as the glass transition temperature, T_g, is approached[1,2]. As the viscosity increases, the

response of the liquid to perturbations decays in a *non-exponential* manner that is often described by a Kohlraush-Williams-Watt (KWW) or stretched exponential,

$$\phi(t) = \phi_o exp\{-(t/\tau)^{\beta}\}, \quad (1)$$

where $0 < \beta < 1$. Meanwhile, the average relaxation time,

$$\tau_{AVG} = \int dt\ exp\{-(t/\tau)^{\beta}\} = \frac{\Gamma(1/\beta)}{\beta}\tau, \quad (2)$$

often increases in a *non-Arrhenius* manner with decreasing temperature to reach a value of τ_{AVG} = 100 seconds just at T_g where the viscosity is approximately 10^{12} Pas. Whereas it is the smallness of the value of β that characterizes the non-exponentiality, the degree of deviation from Arrhenius behavior is usually characterized by the steepness of the increase in τ_{AVG} just near T_g,

$$m = \left.\frac{d\log_{10}\tau_{AVG}}{d(T_g/T)}\right|_{T_g}, \quad (3)$$

a quantity referred to as the *fragility* index[2]. For several decades now, research has suggested the degree by which the melt is both non-exponential and non-Arrhenius depends on the chemical nature of the material and falls within two extremes[3] of either "strong" or "fragile". Fragile liquids (m > 50, β << 1) are primarily comprised of single molecules held together by weak and isotropic van der Waals forces. Strong liquids ($m \leq$ 20, $\beta \approx 1$) are almost exclusively network-forming oxides constructed of discrete covalent bonds.

These two "non's"[4] are also evident in the dynamic structure factor, $S(q,t)$, measured in dynamic light scattering (DLS) studies[5-7]. Near T_g, $S(q,t)$ exhibits a "non-hydrodynamic"[8] (q-independent) relaxation known as the α-relaxation which is well described by the stretched exponential of Eq. 1 with a τ_{AVG} that increases in

proportion with the viscosity. To date, the vast majority of such DLS studies have been limited to reasonably fragile van der Waal fluids whose glass transition occurs near or below ambient temperatures. Few of any studies have investigated the α-relaxation in network-forming melts where T_g occurs at refractory temperatures. This is unfortunate as these network-forming materials possess a rich structural diversity. Not only do many of the networks contain elements of both short and intermediate range order, but the bond connectivity of the network itself can be systematically altered by chemical substitutions[9]. Depending on the oxide, bonding can be either decreased or increased by the addition of alkali oxides and these network-forming structures lend themselves to simple modeling schemes including topological constraint counting[10,11] and discrete bond breaking described by two-level system thermodynamics[12].

In an unprecedented DLS investigation of sodium phosphate melts[13], we were able to study the evolution of the α-relaxation as the connectivity of the network was decreased by the addition of sodium oxide[14]. There we observed a dramatic span of fragilities ranging from $m = 20$ for P_2O_5 with a completely polymerized 3D network of PO_4 tetrahedra to $m = 80$ in the metaphosphate composition ($NaPO_3$) where the de-polymerized structure consists of long chains of tetrahedra[14]. These changes in fragility were accompanied as well by complex variations of $\beta(T)$ with sodium addition. Here, we report findings on a study of sodium borate glass melts. Unlike the de-polymerization wrought by alkali addition in the phosphates, adding sodium to B_2O_3 causes the formation of 4-coordinated boron with an increasing polymerization[15]. Despite some complications with phase separation and crystal nucleation in certain compositional ranges, these first-ever light scattering measurements reveal an α-

relaxation whose non-exponentiality is surprisingly insensitive to polymerization as well as an additional relaxation process linked to the diffusion of sodium ions in the oxide network.

II. Experimental

A. Sample preparation

Samples of $(Na_2O)_x(B_2O_3)_{100-x}$ were prepared from mixtures of anhydrous B_2O_3 (Sigma-Aldrich, 99.98%) and Na_2CO_3 (Sigma-Aldrich, ≥ 99.5%). The carbonate was first recrystallized from a filtered (0.05 micron) aqueous solution in an effort to remove insoluble matter that might contribute unwanted scattering of light. Glass specimens were produced by conventional melting in Pt crucible at 900 to 1000 °C. Homogenization of the melt was achieved by repeated stirring with a Pt rod and proved to be an important step in improving the stability of the melt against crystal nucleation and phase separation. After homogenization, the melt was quenched on brass into the form of a cylindrical ingot and stored in a desiccator for later use.

To conduct the light scattering studies, the ingot was inserted into a pre-cleaned silica ampoule (6 mm ID x 8 mm OD) and remelted in a furnace. After melting, the ampoule was attached to a vacuum line (approximately 100 milliTorr) to de-gas the sample and remove unwanted bubbles from the melt. The ampoule was then quickly transferred to a specially-designed optical oven pre-heated to a desired temperature. The optical oven consists of two stainless steel rods separated by a small (5 mm) gap that have a concentric bore into which the ampoule resides. The outer surface of the rods is

wrapped by nichrome wire and the temperature controlled to within ± 0.1 C during measurements.

B. Photon correlation spectroscopy

Vertically polarized light (532 nm) from a solid state laser (Coherent, Verdi 5) was focused by a lens to illuminate an approximately 50 micron diameter scattering volume in the melt. The light scattered at an angle θ from the forward direction was first passed through a laser line filter to reduce blackbody radiation before being collected by a second lens and imaged onto a 50 micron pinhole located 50 cm in front of a photomultiplier tube (PMT, Thorn EMI 9863/100). Photopulses generated by the PMT were converted to a digital (TTL) equivalent and input to an autocorrelator (correlator.com) which computed the autocorrelation of intensity fluctuations in the scattered light, $C(q,t)$, which is directly related[16] to the dynamic structure factor,

$$C(q,t) = \frac{\langle I_q(t\prime+t) I_q(t\prime)\rangle}{\langle I_q(t\prime)\rangle^2} = 1 + A_{COH}|S(q,t)|^2. \quad (4)$$

Here, the coherence factor, A_{COH}, is an instrumental constant determined by the collection optics and the size of the PMTs photodetector[16] and the scattering wavevector is defined as

$$q = \frac{4\pi n}{\lambda}\sin\frac{\theta}{2}, \quad (5)$$

where n is index of refraction and λ the wavelength of light in a vacuum. Individual correlation functions (or spectra) were collected at a selection of fixed temperatures near and above T_g. Most of the studies were conducted at a scattering angle of $\theta = 90°$ while some measurements (discussed later) where obtained at a series of smaller scattering angles.

III. Results

A. Three regions

Our results are best sorted into three compositional regions with the help of Fig. 1. In melts with x > 22 mol%, the samples were noticeably prone to crystallization that would appear as slowing growing nuclei forming at random locations in the melt. Depending on the severity, some spectra could be obtained before crystals began forming and again after remelting the ampoule in a furnace at temperatures above the liquidus. In this manner, only a limited set of measurements on a sample at x = 24 mol% were obtained.

At compositions between x = 8 mol% to 22 mol%, samples were stable against crystallization but the scattering volume (viewed at magnification through an alignment telescope), while mostly smooth in appearance, exhibited differing levels of granularity. This might be attributed to the existence of a sub-liquidus immiscibility dome reported[18] to exist in this same range of compositions. Although measurements of the α-relaxation could be obtained without phase separation near either edge (x = 10, 12 and 20 mol%), attempts to make measurement near the critical composition (x ≈ 16 mol%) proved to be unfeasible.

Lastly, at low alkali contents below about x = 8 mol%, samples were very stable and the scattering volume appeared smooth and continuous with little or no evidence of any parasitic scattering. In this compositional range, the autocorrelation functions exhibited an unexpected secondary relaxation at times longer than the α-relaxation (see Fig. 2).

B. Two relaxations

Unmodified B_2O_3 exhibits a single, non-exponential α-relaxation[7]. However as shown in Fig. 2, when alkali oxide is introduced at just 2 mol%, an additional relaxation process appears at times longer than the α-relaxation. This second relaxation is reminiscent of the so-called "ultraslow" relaxation reported[19,20] in DLS studies of molecular liquid ortho-terphenyl (OTP): it is nearly exponential and occurs many decades in time after the α-relaxation has occurred. Spectra like that shown in Fig. 2 were thus fit using a two decay model of the form:

$$C(q,t) = 1 + A_{COH}\left|A_F exp\{-(t/\tau_F)^{\beta}\} + A_S exp\{-(t/\tau_S)\}\right|^2, \qquad (6)$$

with a total of 5 fitting parameters. The quality of the fit is excellent (see example in Fig. 2) and unambiguous as the two relaxations are well separated so there is no coupling of the fast and slow parameters. The timescales of the two relaxations increase with decreasing temperature in a nearly Arrhenius fashion (but with some slight curvature) and largely parallel each other (see Fig. 2 inset) remaining about 4 decades apart. As shown in Fig. 3, the amplitude of the slow relaxation is greatest at the lowest alkali content but decreases with increasing sodium and vanishes in the vicinity of x = 10 mol%.

Several clues provide evidence that the primary α-relaxation of the liquid is the faster of the two relaxations. Firstly, when the relaxation times of either process are extrapolated to 100 seconds, it is only the fast relaxation whose temperature at this timescale matches that of the glass transition as measured by others in the literature[11]. Secondly, only the fast relaxation is significantly non-exponential displaying a value of β decreasing from 0.8 to 0.6 as the liquid is cooled. Thirdly, additional studies conducted

using a polarizer added to the collection optics indicate important differences between the two relaxations. With the incident radiation in the vertical polarization state (V), the polarizer allows for study of both the polarized (VV) and de-polarized (VH) scattering to be examined[19]. In the VV configuration we find both relaxations present, but in the VH configuration only the fast relaxation remains. The slow relaxation vanishes in this de-polarized situation which is inconsistent with the α-relaxation. Lastly, additional studies were conducted over a range of scattering angles from θ = 26° to 90° to examine the dependence of the two relaxations on the scattering wavevector. As shown for x = 2 mol% at 583.5 C in the inset of Fig. 3, only the fast relaxation exhibits the q-independence typical of the α-relaxation. The slow relaxation exhibits a strong dependence ($\tau_S \sim q^{-2}$) on the scattering wavevector.

C. The primary α-relaxation

Of the two relaxations, the faster α-relaxation is seen at all compositions including compositions resident in the immiscibility zone (8 < x < 22). The decay is well described by the stretched exponential and curve fitting provides both τ_F and β from which the average relaxation time (Eq. 2) can be determined. Results for the average relaxation time are presented in Fig. 4 and show the increase with decreasing temperature that is characteristic of glass-forming melts. From these data, a short extrapolation to τ_{AVG} = 100 seconds allows for determination of the glass transition temperature. Values of T_g so obtained are reproduced in Fig. 1 and show good agreement with values from the literature[11]. We see that the effect of increasing bonding through the conversion to 4-coordinated boron causes the glass transition temperature to increase suggesting greater

thermal energy is needed to facilitate viscous flow in a network with a higher bond density.

To determine the fragility, we have opted to perform a two-parameter curve fit of the $\tau_{AVG}(T)$ using a modified form of the MYEGA function[21]. The MYEGA function is a recent suggestion for the functionality of the viscosity of melts near T_g inspired by the Adam-Gibb theory[22] that incorporates the fragility index (as it is defined in Eq. 3). In terms of the viscosity, $\eta(T)$, the MYEGA function,

$$\log_{10}\left(\frac{\eta(T)}{\eta_\infty}\right) = (12 - \log_{10}\eta_\infty)\frac{T_g}{T} exp\left\{\left[\left(\frac{m}{12-\log_{10}\eta_\infty}\right) - 1\right]\left[\frac{T_g}{T} - 1\right]\right\} \quad (7)$$

contains three parameters: m, T_g and $\log_{10}\eta_\infty$. By definition, $\log_{10}\eta(T_g) = 12$, while typical values of $\log_{10}\eta_\infty \approx$ -3. Mapping this function over to the relaxation time requires scaling of viscosity by 10^{10} to match $\log_{10}\eta(T_g) = 12$ (in Pa s) with $\log_{10}\tau_{AVG}(T_g) = 2$ and yields

$$\log_{10}\left(\frac{\tau_{AVG}(T)}{\tau_\infty}\right) = (2 - \log_{10}\tau_\infty)\frac{T_g}{T} exp\left\{\left[\left(\frac{m}{2-\log_{10}\tau_\infty}\right) - 1\right]\left[\frac{T_g}{T} - 1\right]\right\}. \quad (8)$$

Curve fitting was performed using just two adjustable parameters (m, $\log_{10}\tau_\infty$) and the results are presented in Fig. 5 along with values of fragility that were reported previously[11] based on analysis of viscosity measurements.

With the exception of compositions in the range x = 8 to 20, the fragility obtained in the current PCS investigation appears to closely match that reported previously. In both cases the fragility increases with increasing bond density and attains fragilities of near 60 similar with the fragility of many organic liquids. However, there is evidence in Fig. 5 that compositions ranging from 8 to 20 are possibly influenced by their trespass into the immiscibility regime. We see that m is generally lower than that in the literature and $\log_{10}\tau_\infty$ deviates substantially from the expected -13 value in this compositional

window. This influence appears to extend also to the stretching exponent which exhibits differing trends depending on whether the composition resides inside or outside the immiscibility window. As shown in Fig. 6, for compositions at low alkali that reside outside the immiscibility range, β decreases on approach toward T_g in a manner that scales with the $\log \tau_{AVG}$ suggesting the stretching is independent of composition and so independent of the changing bond density of the network. By comparison, compositions within the immisciblity zone exhibit a much weaker temperature dependence with $\beta \approx 0.58 \pm 0.06$ nearly constant.

D. The ultraslow relaxation

Having identified the fast relaxation as that viscous relaxation of the melt which reaches timescales of 100 second at T_g, we turn attention now to the origins of the slow relaxation. Firstly, we note that the relaxation timescale of the slow process exhibits a strong dependence on the scattering wavevector, decreasing as the inverse square of q as seen in inset of Fig. 3. In dynamic light scattering, such a wavevector dependence is typical of a *diffusive* process[16] for which the relaxation time is related to the diffusivity, *D*, as

$$\tau_S = \frac{1}{Dq^2}. \qquad (9)$$

Such a diffusive process is not uncommon to photon correlation spectroscopy as spurious slow relaxations can often develop from a variety of scattering artifacts including insoluble debris or small bubbles that happen to migrate through the scattering volume as they diffuse about in the liquid. We offer here three reasons for why the slow relaxation we observe is not an artifact of such parasitic scattering.

Firstly, the slow relaxation we observe is robust in the sense that both it and the α-relaxation develop simultaneously during the collection of the autocorrelation and become more sharply defined as more averaging is performed. This is unlike the behavior when stray, parasitic scatterers wander into the scattering volume. In our experience, such parasitic scatter causes the correlation function to exhibit a secondary decay that develops sporadically and which does not form a reproducible shape. Secondly, we note that the slow relaxation is not present in the x = 0 mol% melt but only appears when sodium is introduced. While this could indicate insoluble matter is present in the sodium carbonate used to batch the glass, it would not explain why the slow relaxation vanishes at compositions above x = 10 mol% (see Fig. 3).

Lastly, we can use the Stokes-Einstein relation, $D = kT/6\pi\eta R$, to make an estimate of the size of any hypothetical particle that might be undergoing Brownian motion so as to cause the slow relaxation. Combining the Maxwell relation, $\tau_F \approx \eta/G_\infty$, that relates the timescale of the α-relaxation to the viscosity and shear modulus (G_∞) with Eq. (9) we obtain the radius of the Brownian particle to be

$$R = \frac{kT}{6\pi\eta D} = \frac{kTq^2}{6\pi G_\infty}\frac{\tau_S}{\tau_F}. \qquad (10)$$

Using T = 700 K as a representative midpoint temperature of our measurements with the ratio of $\tau_S/\tau_F \approx 10^4$ and a typical $G_\infty \sim 10^{10}$ J/m^3, we estimate the necessary particle size to be only $R \sim 0.003$ Å which is unrealistically small. All of these considerations lead us to conclude that the slow relaxation is not a result of the Brownian motion of any parasitic scatterers.

In DLS studies of ortho-terphenyl, Fisher and co-workers observed a very similar ultraslow relaxation appearing some 7 to 9 decades after the primary α-relaxation[19,20].

Unlike the present oxide melts, ortho-terphenyl is a fragile molecular liquid and samples could be produced by careful thermal treatments that did and did not exhibit the slow relaxation, respectively. There too the slow relaxation vanished in a de-polarized scattering experiment and exhibited a strong ($\tau_S \sim q^{-2}$) dependence on the scattering wavevector. Additional studies showed that ortho-terphenyl samples exhibiting the slow relaxation also displayed enhanced static light scattering and the authors concluded both phenomena were the result of long-range density fluctuations: "glassy clusters" with a correlation length of order 100 nm that coexist together with "fluid-like" regions[20].

A slow relaxation was also observed in a recent DLS study of sodium-zinc metaphosphates[23] with low Zn content. There it was suggested that the relaxation might be related to the diffusion of Zn ions as it was demonstrated that the timescale for local ion hopping obtained from measurements of the dc conductivity in a Zn metaphosphate glass closely matched the corresponding relaxation seen in light scattering. To investigate this possible source for the slow relaxation in the present instance, we have computed the diffusivity using Eq. (9) and the plotted the result as a function of inverse temperature in Fig. 7. We see that the diffusivity decreases in a non-Arrhenius manner, decreasing more rapidly just near T_g, but is mostly insensitive to the concentration of Na ions. Included in Fig. 7 are values for the diffusivity of sodium ions obtained by tracer diffusion studies[24] conducted in the solid phase. The fact that these tracer diffusivities nicely extrapolate to meet up with the diffusivities in the melt near T_g as obtained by PCS lead us to conjecture that the slow relaxation is indeed a manifestation of the diffusion of sodium ions within the oxide melt.

IV. Discussion

The PCS measurements reported here demonstrate an α-relaxation in sodium borate melts that is non-exponential and non-Arrhenius over an extensive range of compositions for which the average bond density increases from $\langle n \rangle$ = 3 to $\langle n \rangle$ = 3.3 bridging oxygen per boron atom. Moreover, the relaxation displays an overall increase in fragility with increasing bond density - an increase that runs contradictory to results for sodium phosphate melts[13]. In the phosphates, addition of alkali oxide results in the reduction of bridging oxygens with a corresponding depolymerization of the network from one with $\langle n \rangle$ = 3 bridging oxygen per phosphorous atom to a collection of long polymer chains of PO_4 tetrahedra with $\langle n \rangle$ = 2 at the metaphosphate composition. There, however, the fragility increases as depolymerization proceeds reaching values of m = 80 that are comparable to many van der Waals fluids. Reasons for this descrepancy have been suggested previously and are discussed at some length elsewhere[25].

Of some interest here is the apparent distortion of the α-relaxation wrought by proximity to a subliquidus immiscibility dome in a limited range of compositions. Compositions within the immiscibility window appear to display lower than expected fragility as well as greater non-exponentiality. The reason for this remains unclear and warrants additional studies. However, we do note that in earlier investigations[26,27] of the viscosity of borosilicate melts in which phase separation occurs, an enhancement of the viscosity was reported which was attributed to critical slowing down associated with the second order phase transition near a critical point. It is conceivable that such an enhancement of the τ_{AVG} might likewise cause a lowering of the apparent fragility.

Perhaps the more interesting finding in the present study is the appearance of a secondary relaxation that is attributed to the diffusion of the Na^+ ions in these glass melts. While the addition of alkali oxides to oxide glasses is mainly intended to alter the network structure either by decreasing or increasing the average bridging oxygen bond density, the addition also introduces mobile alkali ions. In the case of sodium borate glasses below T_g, the Na ion is loosely tethered to its charge-compensating BO_4 site in the network and migrates through the network by hopping between adjacent sites. This motion results in frequency-dependent conductivity that is well-documented[28-30] including a dc conductivity related to the diffusivity by the Nernst-Einstein relation

$$\sigma_{DC} = \frac{N(Ze)^2}{kT} D = \frac{N(Ze)^2}{kT} \frac{\xi^2}{6\tau_\sigma}, \tag{11}$$

where N is the ion density, Z the valence, ξ is the hopping distance, and the relaxation time for ion conduction, τ_σ, represents the average time it takes a hop to occur. In studies using broadband dielectric spectroscopy, the ion relaxation also produces a small rise in the dielectric constant ($\Delta\epsilon$) with decreasing frequency of the applied electric field. This increase is thought to reflect the fluctuating dipole associated with hopping of the ion from one BO_4 site to another whose dielectric response mimics the rotation of a permanent dipole of moment $p \sim Ze\xi/2$ for which

$$\Delta\epsilon = \frac{Np^2}{3\epsilon_o kT} = \frac{N(Ze\xi)^2}{12\epsilon_o kT}. \tag{12}$$

Combining this with Eq. (11) above allows the conductivity relaxation time to be determined almost entirely from a measurement of the dc conductivity,

$$\tau_\sigma \approx \frac{\epsilon_o \Delta\epsilon}{\sigma_{DC}}, \tag{13}$$

since the value of $\Delta\epsilon$ is typically of order $\Delta\epsilon \sim 10$.

For a number of years, researchers working to develop glassy solid state electrolytes with high conductivity were interested in understanding the mechanism by which ion motion became "decoupled" from the viscoelastic relaxation of the melt[27,29]. In melts the two relaxations are "coupled" in the sense that the ion relaxation timescale increases along with that of the structural relaxation with $\tau_\sigma \approx \tau_{AVG}$. However, at some point near the glass transition, the ion relaxation separates from the structural relaxation: the network structure begins to freeze while ions can continue to migrate *within* this frozen network by hopping between sites to produce measurable dc conduction. A decoupling index, τ_{AVG}/τ_σ, was introduced[31] to characterize the degree of decoupling and, together with proximity of T_g to ambient temperatures, was often used to engineer glassy solids with high ion conductivity[32].

Our present results add a new perspective to this old theme. At first glance, the two relaxations in the autocorrelation function shown in Fig. 2 would naively suggest two processes that appear strongly decoupled with ion motions occurring far more slowly than the structural relaxation of the network. But this sort of comparison is deceptive as the ionic relaxation decreases with the square of the scattering wavevector while the α-relaxation is independent of scattering wavevector. There is nothing special about the particular q at which our light scattering operates and we emphasize that the two relaxations do share an equivalent timescale at larger wavevectors as illustrated in Fig. 8. At any given wavevector, the timescale of the slow relaxation represents the time for diffusion of ions over a root mean squared displacement, $\sqrt{\langle r^2 \rangle} \sim q^{-1}$, comparable to inverse of the scattering wavevector. We see that as the slow relaxation is extrapolated to higher wavevectors, corresponding to shorter $\sqrt{\langle r^2 \rangle}$, it reaches a value of $\sqrt{\langle r^2 \rangle} \sim \xi$ just

when the timescale would equal that of the structural α-relaxation. This shows that in the melt the diffusion of ions is fundamentally controlled by structural relaxation of the oxide network and the two processes are coupled at many of the temperatures we have investigated. In the case of data for the 8 mol% for which the slow relaxation was measured out to long timescales, both τ_S and τ_F are proportional (therefore coupled) at high temperatures but show decoupling near T_g. This is succinctly demonstrated in Fig. 8 where the slow relaxation has been scaled to a scattering wavevector near ξ^{-1} (i.e., hopping diffusion at the conductivity timescale τ_σ). When adjusted to this shorter length scale, the slow relaxation is seen to coincide with the α-relaxation at high temperatures but begin to decouple from the α-relaxation just in advance of T_g.

The ionic relaxation is a rarity in our PCS experience and one particular puzzle is why this relaxation is only found in certain narrow compositional ranges. Our previous PCS study of sodium metaphosphate melts with 50 mol% sodium, for example, contain a great density of mobile sodium ions but showed no indication of this ion relaxation. By comparison, in the present study the ion relaxation seems most intense at the lowest ion concentrations and then gradually diminishes until it disappears around 10 mol% sodium. It seems then that this relaxation is visible to our light scattering technique only at low alkali concentrations and we believe this may be an inherent feature of how PCS operates.

Light scatters from fluctuations in the dielectric constant of a material[16] and for PCS it is the temporal nature of these fluctuations that lead to time-dependent variations in the scattered intensity of light that can be correlated (as in Eq. (4)) to obtain information regarding the dynamics. In pure B_2O_3, which is void of mobile ions, the

fluctuations of the dielectric constant are generated by density fluctuations of the atoms that comprise the network and give rise to the α-relaxation we observe; a measure of dynamic structure factor equivalent to the time-dependent density-density autocorrelation function. The strength of the scattering is proportional to the average square of the fluctuations in the dielectric constant and is generally rather weak in glassy liquids as it is limited by the small size of the corresponding fluctuations in density. However, when we introduce the sodium ions, along with the BO_4 sites they tether to, we create a rather large permanent dipole that can fluctuate substantially when the ion undergoes a hop to a neighboring site. Again, the strength of light scattering from this new object depends on the size of the dielectric constant fluctuation it produces *relative to its average*. At low concentrations, the dielectric constant averaged over a small collection of sodium ion/BO_4 dipoles is small allowing the *fluctuation* to be relatively large in contrast. A large signal-to-noise is thus realized for this particular scattering process resulting in a substantial contribution to the PCS correlation function. We speculate that at higher concentrations, this contrast is weakened as the average dielectric constant due to the dipoles increases reducing the signal-to-noise of the fluctuation and diminishing the contribution to the autocorrelation function.

In summary, our light scattering investigations of network-forming oxides represent something of a new avenue in the study of glass dynamics wherein the effects of structural modifications and changing bond density can be systematically studied. In addition to expected features of the primary viscous relaxation, the findings of a relaxation process associated with ion diffusion opens up the possibility of further investigations of these alkali-modified oxides to better understand the mechanisms by

which ions migrate within the network. Of particular interest may be the presence of two dissimilar alkali, say sodium and potassium, for which dramatic decreases in dc conductivity are known to occur[33].

Acknowledgement: This material is based upon work supported by the National Science Foundation under Grant No. (DMR2051396).

References

1. M. D. Ediger, C. A. Angell and S. R. Nagel, Supercooled liquids and glasses, J. Phys. Chem. 100(31): 13200-13212 (1996).

2. P. G. Debenedetti and F. H. Stillinger, Supercooled liquids and the glass transition, Nature 410(6825): 259-267 (2001).

3. R. Bohmer, K. L. Ngai, C. A. Angell and D. J. Plazek, Non-exponential relaxations in strong and fragile glass formers, J. Chem. Phys. 99(5):4201-4209 (1993).

4. J. C. Dyre, Colloquium: The glass transition and elastic models of glass-forming liquids, Rev. Mod. Phys. 78:953-972 (2006).

5. G. Fytas, C. H. Wang, D. Lilge and T. Dorfmuller, Homodyne light beating spectroscopy of o-terphenyl in the supercooled liquid state, J. Chem. Phys. 75(9): 4247-4255 (1981).

6. D. L. Sidebottom and C. M. Sorensen, Light scattering study of the glass transition in salol, Phys. Rev. B 40(1): 461-466 (1989).

7. D. Sidebottom, R. Bergman, L. Borjesson and L. M. Torell, Two-step relaxation decay in a strong glass former, Phys. Rev. Lett. 71(4):2260-2263 (1993).

8. R. D. Mountain, Thermal relaxation and Brillouin scattering in liquids, J. Res. Nat. Bur. Stand. Sect. A 70, 207-220 (1966).

9. Zarzycki J. Glasses and the vitreous state. Cambridge: University Press; 1991.

10. He H, Thorpe MF. Elastic properties of glasses. Phys. Rev. Lett. 1985; 54(19): 2107 – 2110.

11. J. C. Mauro, P. K. Gupta and R. J. Loucks, Composition dependence of glass transition temperature and fragility. II. A topological model of alkali borate liquids, J. Chem. Phys. 130(23): 234503 (2009).

12. C. A. Angell and K. J. Rao, Configurational excitations in condensed matter and the "bond lattice" model for the liquid-glass transition, J. Chem. Phys. 57(1): 470-481 (1972).

13. R. Fabian, Jr. and D. L. Sidebottom, Dynamic light scattering in network-forming sodium ultraphosphate liquids near the glass transition, Phys. Rev. B 80(6): 064201 (2009).

14. R. K. Brow, Review: the structure of simple phosphate glasses, J. Non-Cryst. Solids 263&264:1-28 (2000).

15. P. J. Bray and J. G. O'keefe, Nuclear magnetic resonance investigations of the structure of alkali borate glasses, Phys. Chem. Glasses 4(2): 37-46 (1963).

16. Berne, B. J. and Pecora, R. *Dynamic Light Scattering* (John Wiley & Sons, New York, 1976).

17. D. L. Sidebottom, Dynamic Light Scattering in *Characterization of Materials* ed. by Elton N. Kaufmann (John Wiley & Sons, 2012).

18. R. R. Shaw and D. R. Uhlmann, Subliquidus immiscibility in binary alkali borates, J. Am. Ceram. Soc. 51(7):377-382 (1968).

19. A. Patkowski, H. Glaser, T. Kanaya and E. W. Fischer, Apparent nonergodic behavior of supercooled liquids above the glass transition temperature, Phys. Rev. E 64:031503 (2001).

20. A. Patkowski, Th. Thurn-Albrecht, E. Banachowicz, W. Steffen, P. Boseche, T. Narayanan, and E. W. Fischer, Long-range density fluctuations in orthoterphenyl as studied by means of ultrasmall-angle x-ray scattering, Phys. Rev. E 61(6): 6909 - 6913 (2000).

21. J. C. Mauro, Y. Yue, A. J. Ellison, P. K. Gupta and D. C. Allan, Viscosity of glass-forming liquids, Proc. Natl. Acad. Sci. U.S.A. 106:19780-84 (2009).

22. Adam G, Gibbs JH. On the temperature dependence of cooperative relaxation properties in glass-forming liquids. J. Chem. Phys. 1965; 43: 139 – 146.

23. D. L. Sidebottom and D. Vu, Assessing the network connectivity of modifier ions in metaphosphate glass melts: A dynamic light scattering study of Na-Zn mixtures, J. Chem. Phys. 145: 164503 (2016).

24. Y. H. Han, N. J. Kreidl and D. E. Day, Alkali diffusion and electrical conductivity in sodium borate glasses, J. Non-Cryst. Solids 30:241-252 (1979).

25. Sidebottom DL. Fragility of network-forming glasses: A universal dependence on the topological connectivity. Phys. Rev. E 92, 062804 (2015).

26. J. H. Simmons, A. Napolitano and P. B. Macedo, Supercritical viscosity anomaly in oxide mixtures, J. Chem. Phys. 53: 1165 - 1170 (1970).

27. J. H. Simmons and P. B. Macedo, Viscous relaxation above the liquid-liquid phase transition of some oxide mixtures, J. Chem. Phys. 53(7):2914-2922 (1970).

28. C. A. Angell, Dynamic processes in ionic glasses, Chem. Rev. 90:523-542 (1990).

29. D. L. Sidebottom, Colloquium: Understanding ion motion in disordered solids form impedance spectroscopy scaling, Rev. Mod. Phys. 81:999-1014 (2009).

30. D. L. Sidebottom, Universal approach for scaling the ac conductivity in ionic glasses, Phys. Rev. Lett. 82(18):3653-3656 (1999).

31. C. A. Angell, Fast ion motion in glassy and amorphous materials, Solid State Ionics 9&10: 3-16 (1983).

32. H. K. Patel and S. W. Martin, Fast ionic conduction in Na2S+B2S3 glasses: Compositional contributions to nonexponentiality in conductivity relaxation in the extreme low-alkali-metal limit, Phys. Rev. B 45, 10292 - 10300 (1992).

33. M. D. Ingram, The mixed alkali effect revisited: A new look at an old problem Glastech. Ber. Glass Sci. Technol. 67(6) 151-155 (1994).

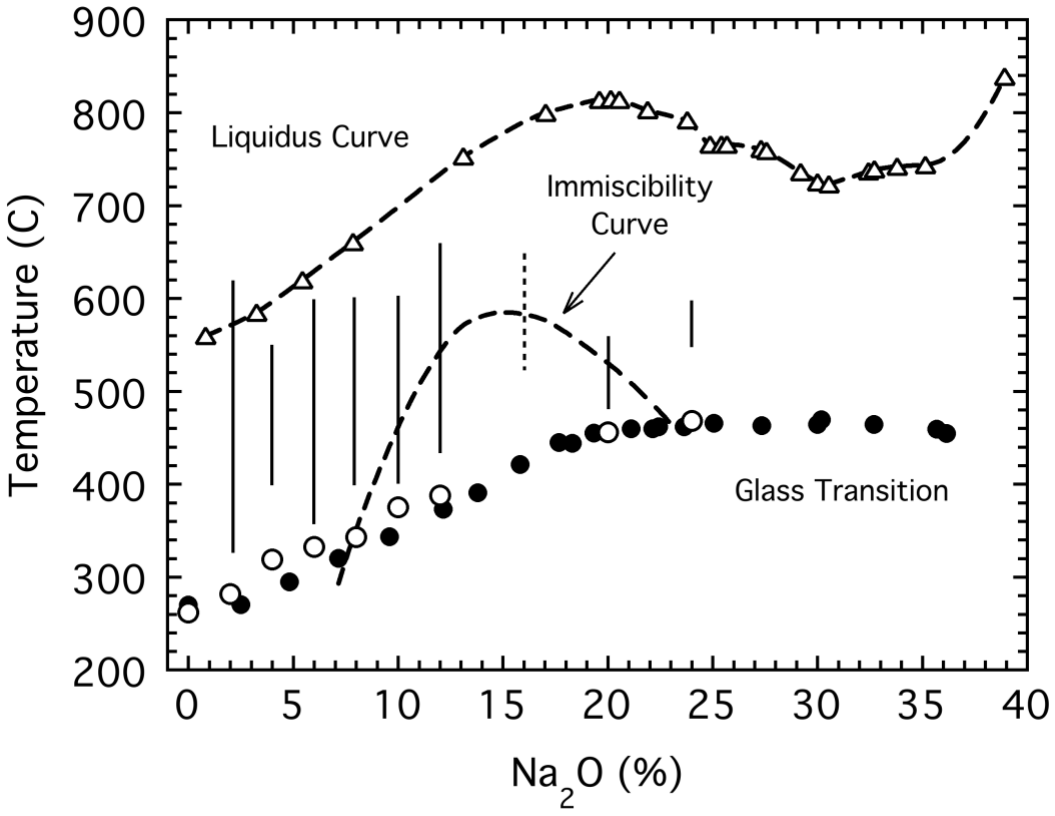

Fig. 1 Map of transitions occurring in sodium borate melts including both the liquidus curve (triangles) and the glass transition temperature as reported in the literature[11] (solid circles) and as determined from the present measurements (open circles). Dashed curve is the immiscibility dome reported in reference[18]. Vertical lines indicate ranges over which PCS measurements were conducted. Measurements attempted for x = 16 mol% (dotted line) were inconclusive and are not discussed.

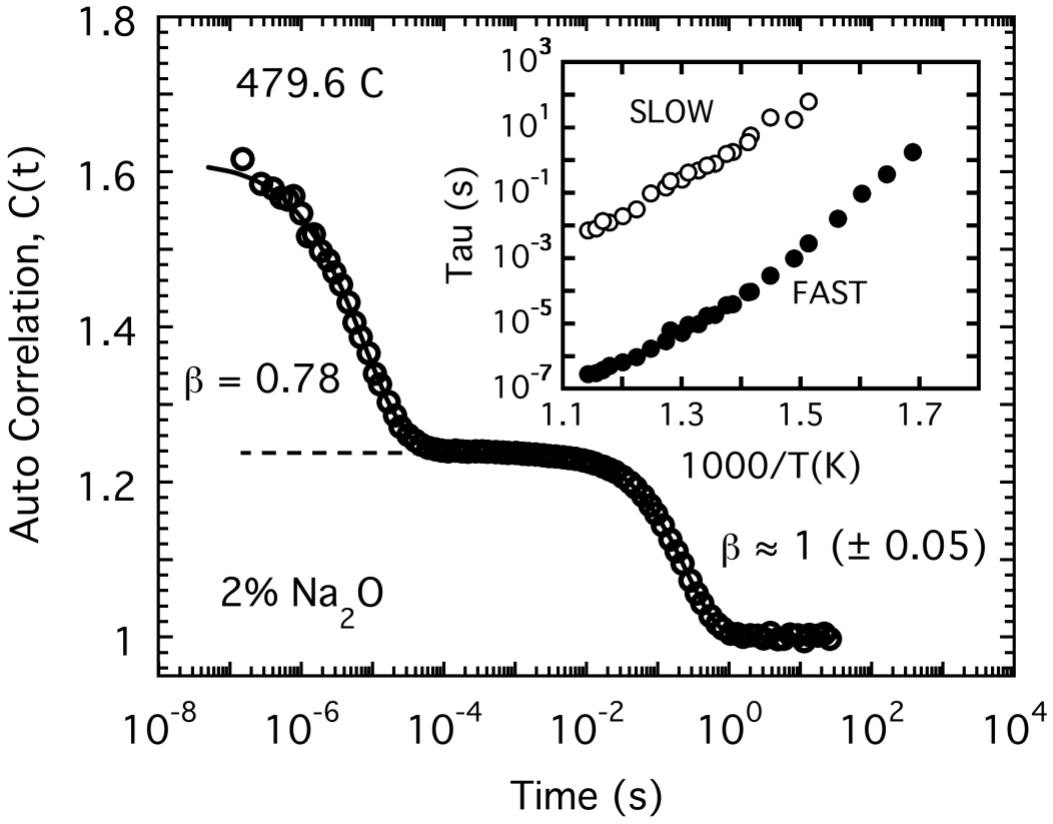

Fig. 2 Autocorrelation function recorded at 479.6 C for a sample with x = 2 mol% sodium oxide shows two relaxations: a fast, non-exponential decay followed some four decades later by a slower nearly exponential decay. Relaxation times (τ_S and τ_F) determined by fitting to Eq. (6) are plotted in the Arrhenius fashion in the inset.

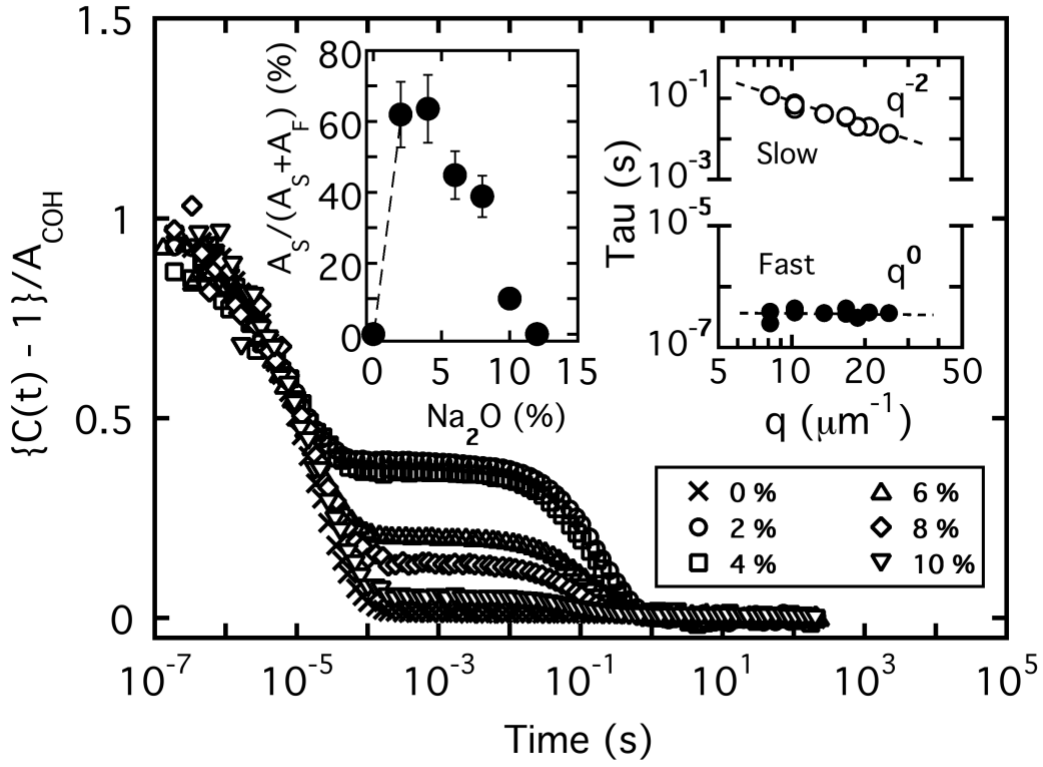

Fig. 3 Selected spectra with approximately common relaxation times are plotted together to illustrate the systematic changes in the amplitude of the slow relaxation. Left inset: Ratio of the slow relaxation to the total relaxation amplitude shows that the slow relaxation is only present when alkali ions are introduced and vanishes for compositions with more than x = 10 mol% alkali oxide. Right inset: The two relaxations (x = 2 mol%) exhibit different dependences on the scattering wavevector suggesting the slow relaxation is a diffusive process.

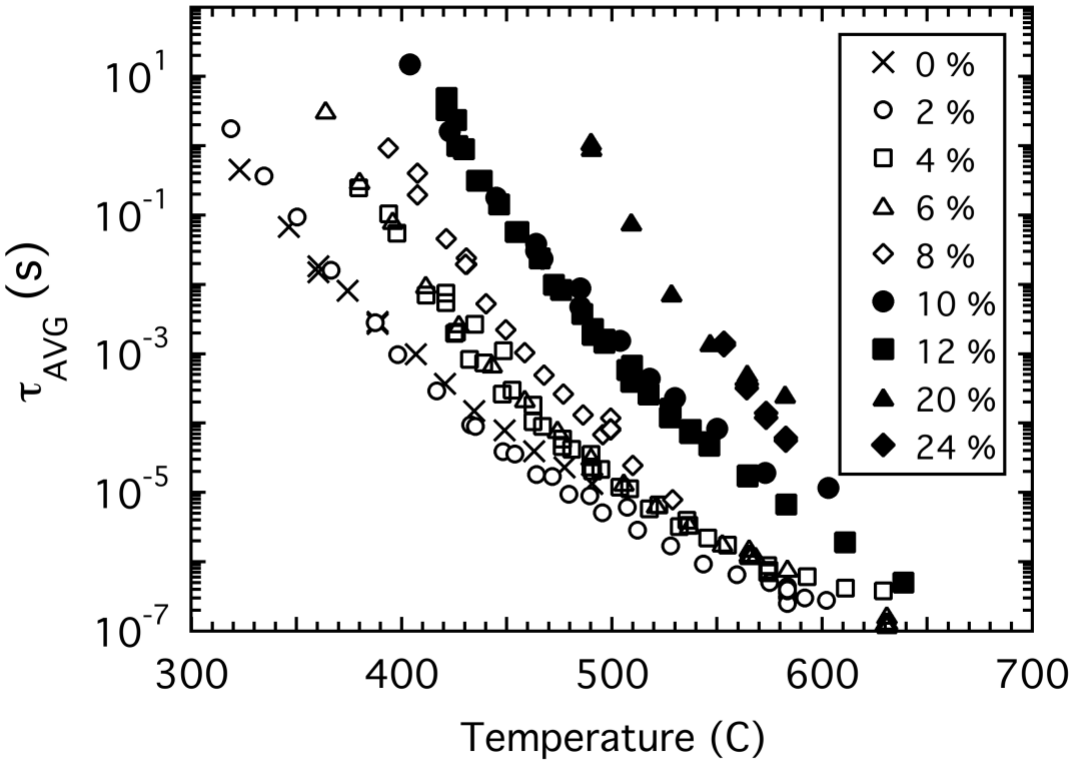

Fig. 4 Average relaxation time for the (fast) α-relaxation as a function of temperature.

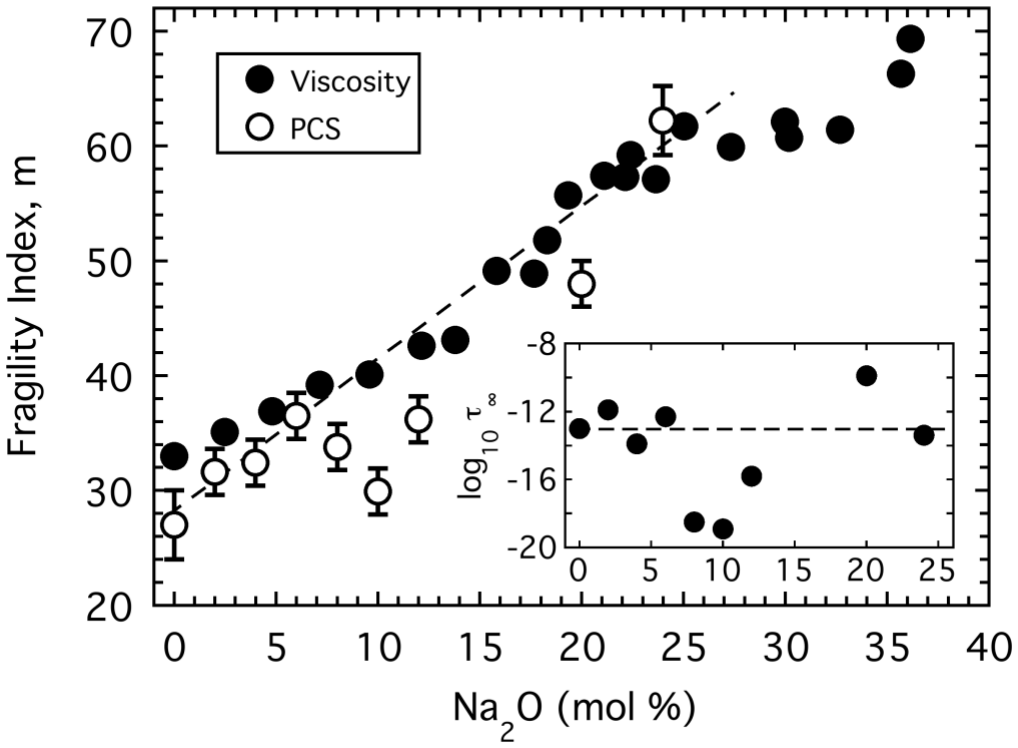

Fig. 5 Fragility of sodium borate melts as reported from analysis of viscosity[11] and from fitting PCS findings of τ_{AVG} to Eq. (8). Dashed line indicates enhanced agreement for compositions that reside outside the immiscibility window. Inset: Values of $\log_{10} \tau_\infty$ obtained from fitting to Eq. (8) also exhibit deviations from the anticipated value (dashed line) for compositions within the immiscibility window.

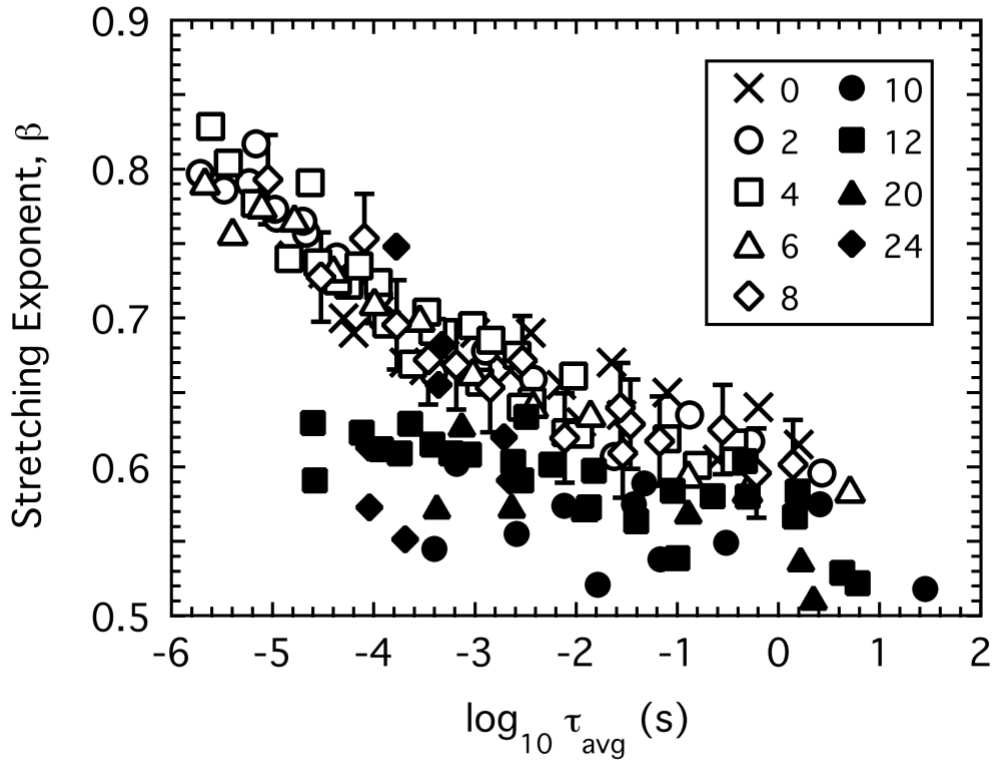

Fig. 6 Stretching exponent of the α-relaxation as measured by PCS as a function of the $\log_{10}\tau_{AVG}$. For compositions below x = 10 mol% that reside outside the immiscibility window, $\beta(\log_{10}\tau_{AVG})$ collapses to a common curve indicating that non-exponentiality is dependent only on proximity to the glass transition point. Compositions above x = 10 mol% deviate from this scaling curve.

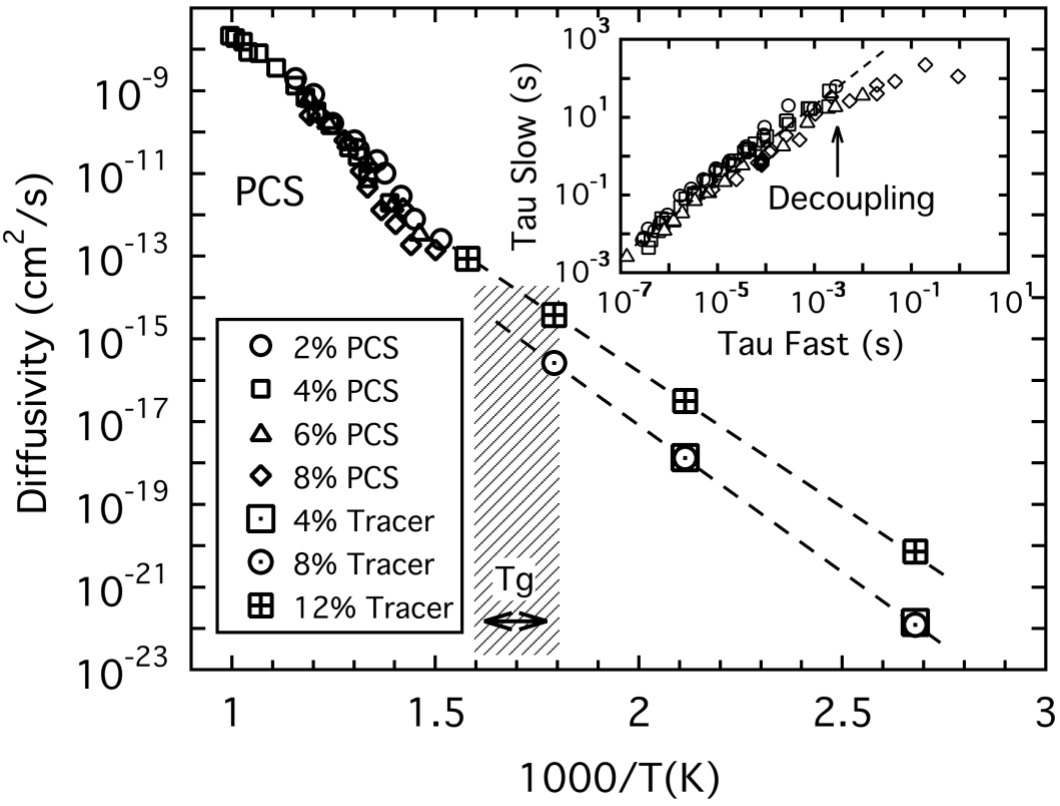

Fig. 7 The diffusivity of sodium ions as measured by tracer diffusion[24] in the solid and the diffusivity of the slow relaxation measured in melts by PCS appear to merge smoothly near T_g suggesting the slow process involves the diffusion of the sodium ion. Inset: A plot of the slow relaxation time against the fast relaxation time shows the two are proportional but may begin to decouple just near T_g.

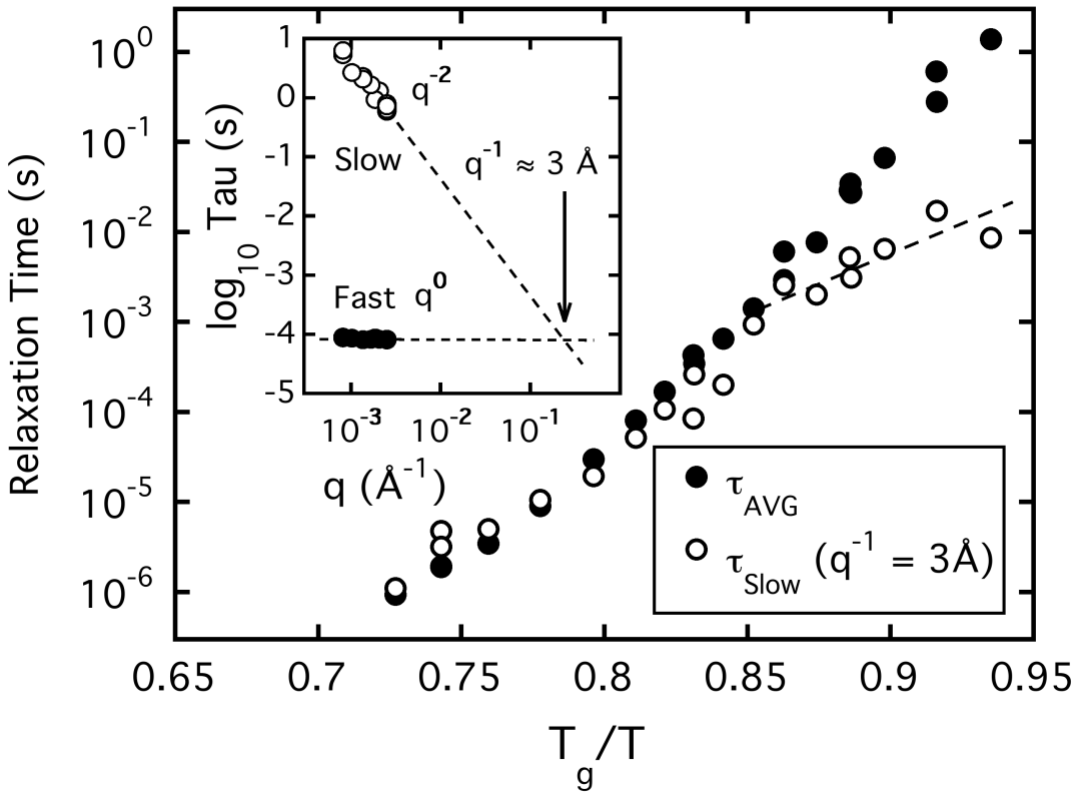

Fig. 8 Inset: The slow and fast relaxations (8 mol%) share a common timescale only for a length scale of a few Angstroms where ions undergo a hopping between neighboring sites. Main: When the slow relaxation is rescaled to correspond with this same hopping length, its timescale matches that of the α-relaxation except just near T_g where the ionic relaxation begins to become "decoupled" in advance of the solidification of the melt.